



# In situ spectroelectrochemical measurements during the electro-oxidation of ethanol on WC-supported Pt-black. Part II: Monitoring of catalyst aging by in situ Fourier transform infrared spectroscopy

Benedetto Bozzini<sup>a,\*</sup>, Gian Pietro De Gaudenzi<sup>b</sup>, Abderrahmane Tadjeddine<sup>c</sup>

<sup>a</sup> Dipartimento di Ingegneria dell'Innovazione, Università del Salento, Via Monteroni, I-73100 Lecce, Italy

<sup>b</sup> Films S.p.a., v. Megolo 2, I-28877 Anzola d'Ossola, Italy

<sup>c</sup> UDIL, Bat. 201P1, CNRS, Univ. Paris-Sud, BP 34, 91898 Orsay, France

## ARTICLE INFO

### Article history:

Received 19 March 2010

Received in revised form 4 June 2010

Accepted 7 June 2010

Available online 15 June 2010

### Keywords:

FT-IR

Electrocatalyst

WC

Pt

Degradation

## ABSTRACT

As a continuation of a project on the spectroelectrochemical analysis of long-term behaviour of WC-supported Pt electrocatalysts (for SFG results, see part I: [1]), in this paper we report in situ FT-IR spectroscopy experiments, carried out during prolonged electro-oxidation of ethanol on Pt-black. From the analytical point of view, as expected, FT-IR spectra showed the presence of adsorbed acetic acid and ethanol, in addition to the well-known, dominant species: linearly adsorbed CO (2044–2063  $\text{cm}^{-1}$ ) and solution-phase CO<sub>2</sub> (2345  $\text{cm}^{-1}$ ). As far as quantitative spectroscopic results are concerned, a notable sensitivity of the interfacial chemistry to catalyst aging could be highlighted by this approach. The spectra recorded in three subsequent series of potential-cycling experiments showed a clear-cut dependence of spectral patterns and peak intensities, on the applied potential and on the oxidation duration. Qualitative spectral changes seem to suggest – coherently with in situ SFG results obtained with the same system [1] – that electrocatalyst aging correlates with a higher surface coverage with ethanol as compared with acetic acid. Quantitative analysis, based on fitting with Lorentzian lineshapes, yields information that can be used as a molecular-level diagnostic of the modification of the catalyst–adsorbate structure.

© 2010 Elsevier B.V. All rights reserved.

## 1. Introduction

The development of proton-exchange membrane fuel cells (PEMFCs) for power generation has brought to the limelight new challenges related to the durability of materials. Among them, the degradation of the widely used carbon-supported Pt-based catalysts is becoming a key point that calls for the introduction of alternative materials, with improved long-term resistance to catalyst agglomeration and support corrosion, in addition to the more extensively investigated poison-tolerance. Being characterised by good electronic conductivity, resistance to acidic environment, low cost and outstanding mechanical properties – in addition to some degree of electrocatalytic behaviour towards hydrogen oxidation – tungsten carbide (WC) has been recently indicated as a possible candidate to replace the traditional carbon support [2–11]. CO poisoning during the electro-oxidation of hydrogen at WC was studied in [2] and found to be limited and reversible. Furthermore, the addition of WC to Pt [3], Pt–Ru [3], Pd [9,11] and Au–Pd [10]

catalysts to improve the tolerance to CO during ethanol oxidation has been proved. The prospective combination of WC with metals not belonging to the platinum metal group has been pointed out as appealing for economical consideration: improved catalytic behaviour was found for nanocrystalline WC, as such and in combination with Ag [4]. Furthermore, the combination of WC with CNT has proved effective in enhancing the electrocatalytic activity in Pt–WC catalysts for ethanol oxidation in alkaline media [11].

As far as thermal and electrochemical stability are concerned, a comparative study on WC- and C-supported Pt was carried out in [5]. The two supports were loaded with comparable amount of Pt and subjected to several oxidation cycles: WC was found to be more stable than commercial carbon supports. Moreover, it is worth noting that Pt–WC and Pt–WC/C have been proposed as cathodic catalysts for oxygen reduction [8] and hydrogen production by methanol electrolysis [9].

This work is part of a long-term project aimed at understanding catalyst degradation at the molecular level. The combination of materials we chose to set up the methodology is using WC supports for the reasons stated in the above paragraph and Pt electrocatalyst. Of course, Pt is not the optimal material for advanced alcohol electrocatalysis, but we regard this metal – prepared in various forms – as a benchmark case for our study. In particular, within the scope

\* Corresponding author. Tel.: +39 832 297323; fax: +39 832 297323.

E-mail addresses: [benedetto.bozzini@unile.it](mailto:benedetto.bozzini@unile.it), [benedetto.bozzini@unisalento.it](mailto:benedetto.bozzini@unisalento.it) (B. Bozzini).

of this project, we have considered Pt-black as a standard and electrodeposited Pt as a more flexible approach, especially intended as the possible preparation method of choice for nanostructured supports (e.g. [12]). In a previous paper [1], we studied the behaviour of WC-supported Pt-black during the prolonged electro-oxidation of ethanol by in situ VIS-IR Sum Frequency Generation (SFG) spectroscopy. In subsequent papers, we shall report in situ FT-IR and SFG results on catalysts obtained by electrodepositing Pt nanoparticles onto WC. The present research is based on the use of FT-IR spectroscopy that – due to its extreme sensitivity to the interfacial conditions of adsorbed CO, combined to the capability of detecting subtle changes in surface composition with molecular specificity – is ideal for the monitoring and identification of support-catalyst modifications under prolonged usage. The authors are not aware of previous in situ electrochemical FT-IR work carried out with WC-supported Pt and believe that this work will contribute both to the molecular-level understanding of catalyst degradation processes in general and of the peculiarities of this novel, promising catalyst support, in particular.

## 2. Materials and methods

### 2.1. Electrode preparation

The catalyst layer was prepared according to the procedure described in [1,13]: an ink composed of 0.2 g of Pt-black (Aldrich), 0.7 g of Nafion solution (Aldrich 31175-20-9 5 wt.% in mixture of lower aliphatic alcohols and water) and 4 mL of isopropyl alcohol was sonicated for 1 h. A few drops were cast on the surface of a polished WC electrode and dried under  $N_2$  flow.

### 2.2. Electrolyte

The composition of the solution employed in our work was: 0.1 M EtOH (Aldrich), 0.1 M  $HClO_4$  (Fluka). All the solutions were prepared from analytical grade reagents and Millipore water with resistivity  $>18 M\Omega cm$ .

### 2.3. In situ IR spectroscopy

Subtractively normalised interfacial Fourier transform infrared (SNIFT-IR) measurements were carried out with a Nicolet NEXUS, equipped with an MCT-High D\* detector cooled by liquid nitrogen. p-Polarised light was used, obtained with a ZnSe Au wire grid polarizer. The beam path of the FT-IR spectrometer was continuously purged with a Parker Balston 75-52-12VDC  $CO_2$  remover/air dryer system. The resolution of the spectrometer was set to  $8 cm^{-1}$ . A thin-layer device – described in [14–16] – was employed for in situ work. The working electrode was pressed against a  $CaF_2$  prismatic  $60^\circ$  IR-window. The cell was located in the beam path of a VeeMax mirror system, with reflection angle set at  $60^\circ$ . Before each measurement, the solution was deaerated by nitrogen bubbling for 20 min and then kept under a nitrogen blanket during the measurement of spectra.

Electrochemical measurements were performed with an AMEL 5000 programmable potentiostat. The reference electrode was an RHE, all potentials are reported on the RHE scale. A scan rate of  $0.05 V s^{-1}$  has been employed in voltammetric experiments.

## 3. Results and discussion

Cyclic voltammetry work on this system has already been published in [1]; here we summarise the essential outcomes for the readers' perusal. (i) The bare WC electrode does not exhibit any appreciable electrocatalytic behaviour vs. ethanol. (ii) When the

WC electrode, functionalised with Pt-black, is immersed in the solution containing only 0.1 M  $HClO_4$ , we observe a voltammetric behaviour that is very similar to that of a Pt electrode in acidic solution, in terms of hydrogen evolution and Pt oxidation. Moreover, a Tafel-type current due to the oxidation of the WC substrate is observed at potentials more anodic than 1.05 V. (iii) In the case of 0.1 M  $HClO_4$  + 0.1 M EtOH solution, two peaks were observed in the anodic scan, around 0.6 V and 0.85 V. According to the interpretation provided in [17], these peaks can be related to ethanol oxidation by: (a)  $OH_{ads}$  onto a Pt(I) intermediate state and (b) PtO, respectively. We can thus conclude that the behaviour of the WC–Pt system, in the relevant potential range, shows the essential characteristics of Pt-based electrodes.

We carried out potentiostatic FT-IR measurements on a WC–Pt-black electrode prepared as described in Section 2.1. We scanned the potential anodically in the range +0.500 V to 1.050 V. The reference potential for spectral ratioing was set either to +0.050 V. We repeated the experiment three times in order to gain information on the aging of the electrocatalyst. Between the replicated applications of the anodic potential staircase, the potential was held at +0.65 V in the ethanol oxidation range, but well cathodic with respect to WC oxidation (for details, see v. SFG [1]) for 12 h. Before resuming the FT-IR measurements, the reacted electrolyte was removed and substituted with a fresh aliquot. The electrode was not subjected to any treatment and was not removed from the spectroelectrochemical cell. This aging process led to morphological changes, that can be detected by SEM: typical micrographs of electrocatalyst at the beginning and end of the treatments described in this work are shown in Fig. 1(1) and (2), respectively: the most notable structural result of electrode aging was particle agglomeration (feature  $\alpha$ ), accompanied by the formation of some bare support areas (feature  $\beta$ ). The observable spectral patterns found in the three successive replicate experiments (henceforward referred to as experiments A, B and C) are essentially the same and are coherent with the literature [18–26], while electrode aging gives rise to marked quantitative differences.

Three chief types of IR bands could be measured, corresponding to: (i) adsorbed CO (ca.  $2050 cm^{-1}$ ), (ii) other ethanol oxidation products (range ca.  $1200$ – $1300 cm^{-1}$ ) and (iii) liquid-phase  $CO_2$  (ca.  $2350 cm^{-1}$ ). Details on the spectral patterns and their dependence on electrocatalyst aging are provided below. As customary (e.g. [19]), each background-subtracted IR band  $I(\nu)$  ( $\nu$  denoting the wavenumbers), has been fitted with a Lorentzian lineshape:  $I(\nu) = (2/\pi) \cdot A \cdot W / (4(\nu - \nu_0)^2 + W^2)$ , where  $\nu_0$  is the peak position,  $A$  – the peak area – is proportional to the oscillator intensity and  $W$  represents the peak width.

### 3.1. CO stretching range

In the wavenumber range of the stretching of linearly adsorbed CO  $\nu(CO)$  (ca.  $2050 cm^{-1}$ ), the prototypical negative band is found, corresponding to the widely documented ethanol oxidation intermediate (Fig. 2). The  $\nu(CO)$  band exhibits peak position, Stark-tuning (Fig. 3(1)) and peak area  $A$  (Fig. 3(2)) that are a function of electrode aging, while the peak width  $W$  (Fig. 3(3)) does not seem to be measurably affected by potential cycling and prolonged ethanol oxidation. The Stark-tuning has been evaluated by weighted linear least squares regression, using the 95% confidence intervals derived from the Lorentzian fit as weights.

As it can be observed in Fig. 3(1), both the peak position and the Stark-tuning tend to decrease systematically with electrode aging. In the literature regarding in situ vibrational spectroscopies (chiefly IR and SERS) of electrochemical adsorption of CO onto different single-crystal and polycrystalline electrodes, the Stark-tuning of the  $\nu(CO)$  stretching band has been measured and discussed from a variety of points of view. Adequate physical interpretations of

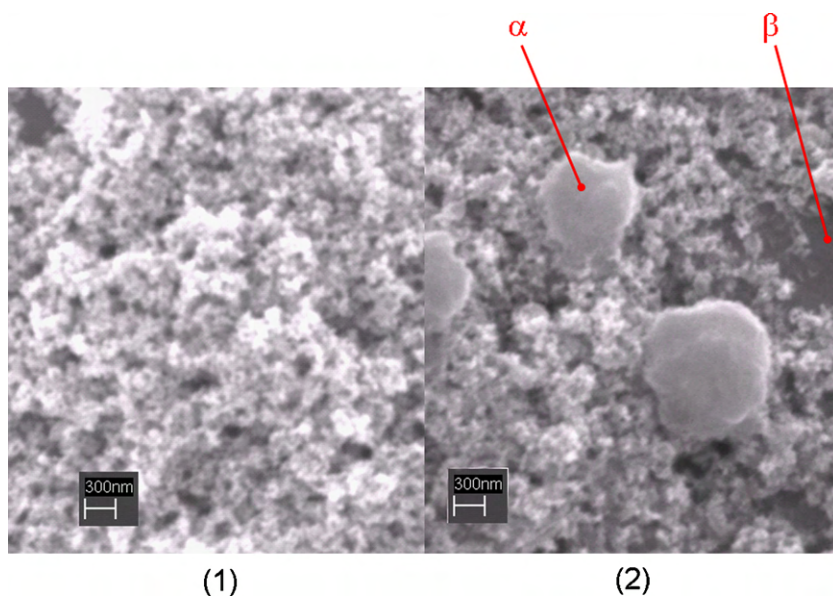


**Fig. 1.** SEM micrographs of WC/Pt-black electrode in pristine conditions (1) and after the three anodic potential sequences described in this work (2).  $\alpha$  and  $\beta$ : chief morphological changes induced by the aging process.

the Stark-tuning of adsorbed CO during prolonged oxidation of ethanol can in principle provide notable insight into the evolution of the electrocatalyst properties. In fact, the band position and respective Stark-tuning are sensitive to the metal–adlayer structure and any effect relevant to the adsorbate; the adsorbing surface of their interaction can affect these observables. As far as linear Stark-tunings are concerned, the band position  $\nu$  of an intramolecular stretching of an adsorbed molecule as a function of the electrode potential  $V$  under given adsorption conditions, can be written as  $\nu(V) = A + B_{BE} + C \cdot V$ . For the case of non-linear potential dependence, relevant information can be found in [1]. In this equation  $A$  is the free-molecule value,  $B_{BE}$  is the potential-independent shift accounting for binding-energy (BE) effects due to adsorption and the coefficient  $C$  can be regarded as due to the combination of two types of effects: (i) related to the molecular properties of the adsorbate and (ii) connected to the coupling between adsorbates, due to either molecular packing or coadsorption. In principle, type-i

effects convey information of the variation of the singleton frequency of the adsorbate as a function of the interfacial electric field. In fact, potential-dependent chemical bonding can be anticipated, due to varying metal–adsorbate orbital overlap. In addition, type-i contributions to  $C$  would give indirect information on the electronic structure of the metal, through the formation of adsorption bonds [27,28]. As far as the physical interpretation of type-i processes, ASED-MO (atom superposition and electron delocalisation molecular orbital) method has been shown to provide some insight. In fact, the ASED-MO method [29–31] consists in a semi-empirical bonding approach based on a model involving partitioning of the molecular and electronic charge distribution functions for a suitable cluster of metal atoms into “rigid atomic” and “delocalised” components, yielding repulsive and attractive potential energy contributions, respectively. The alteration of the electrode potential is accounted for by varying the valence-state ionisation potential of the metal atoms and hence the metal surface electronic energy. These ener-

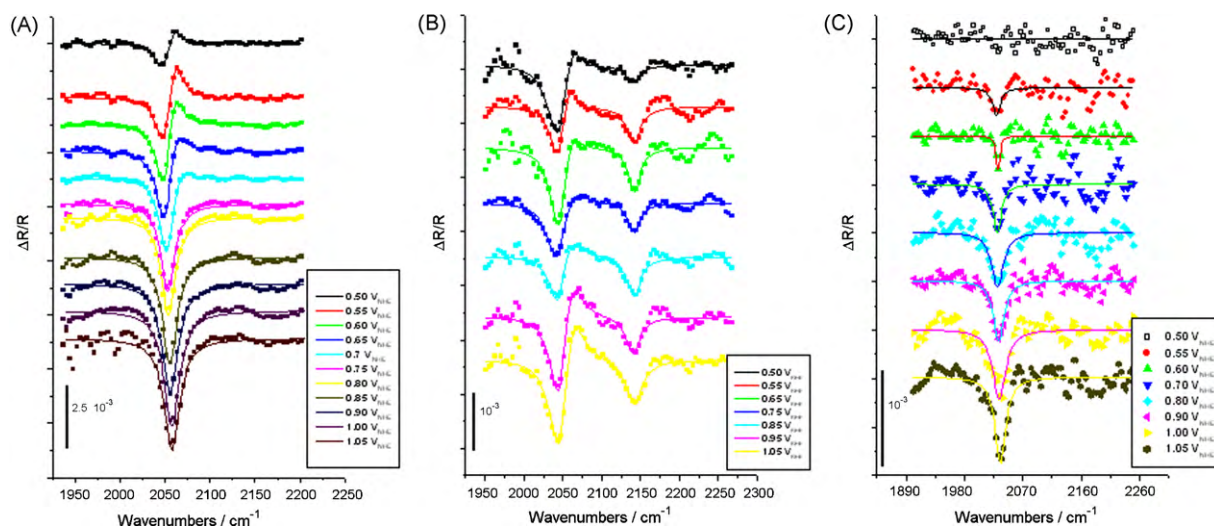


**Fig. 2.** Potential-dependent in situ FT-IR spectra measured at the indicated potentials on a WC/Pt-black electrode in contact with a 0.1 M  $\text{HClO}_4$  + 0.1 M  $\text{CH}_3\text{CH}_2\text{OH}$  solution; reference spectrum measured at 0.05  $V_{\text{RHE}}$ . Wavenumbers range corresponding to CO stretching. (A) First sequence, (B) second sequence, and (C) third sequence.



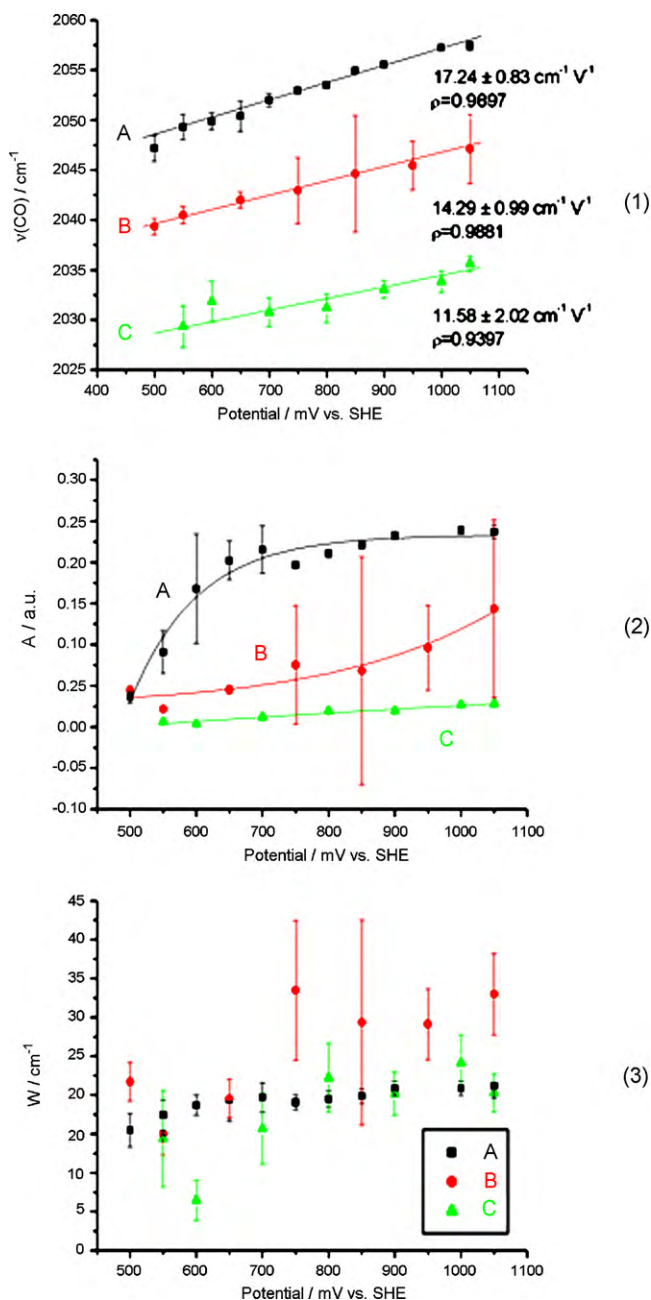


**Fig. 3.** Lorentzian fit parameters of the linearly adsorbed CO stretching peaks reported in Fig. 2, with respective 95% confidence intervals. (1) Peak position  $\nu_0$ , (2) peak area  $A$ , (3) peak width  $W$ . (A) First sequence, (B) second sequence, and (C) third sequence.

getic alterations affect the degree of adsorbate–surface orbital mixing [29]. A decrease of potential would thus be associated with increased back-donation. Within this framework, a decrease of electrode potential is predicted to give rise to an increase in back-donation causing in turn a reduction of the band frequency [31]. Ab initio MO computation of the Stark-tuning has also been carried out for CO adsorbed onto Cu [32,33] and Pd [34] clusters. Doubts on the universality of the back-donation effects in explaining Stark-tuning have been raised in [34], where electrostatic effects have been invoked to explain the experimental results obtained with Pd. MO computations predict substantial field-induced charge-flow from the metal to the ligand, the extent of back-donation increasing markedly towards more negative charges. The origins of the cou-

pling effects accounted for in type-ii contributions to  $C$  are mutual dipolar-field and other vibrational interactions within the array of adsorbate oscillators. This coefficient is expected to be sensitive to island formation, inter-adsorbate distances and effective electronic and vibrational polarisabilities. The interaction between nearby adsorbates may stem from two principal physical effects: the dynamic dipole–dipole coupling and the static chemical interaction involved primarily through-metal bonding effects [35]. The dynamic contribution must be positive, while the static one can be either positive or negative [36], but since the modulus of the static contribution is smaller than that of the dynamic one [37], the overall effect should give rise to positive  $C$  values. Very similar Stark-tuning rates have been measured for CO adsorption onto Pd, Pt, Ir and Rh, but different values have been recorded with acid vs. alkaline electrolytes, denoting different interactions of the adsorbates with the electrochemical environment [38]. Data on the dependence of  $d\nu(\text{CO})/dV$  on the applied potential  $V$  have been reported in [29] for Pt(1 0 0), Pt(1 1 0), Pt(1 1 1), Rh(1 1 1) and Rh(1 0 0). The Stark-tuning has been shown to increase as the coverage decreases. Coadsorption effects can thus be accounted for through type-ii contributions to the parameter  $C$ . Site occupancy changes and surface coordination geometry have been reported for Pt–CO as an effect of  $\text{H}_2\text{O}$  and  $\text{H}$  coadsorption [29]. Qualitatively different coadsorption-induced potential-dependent surface coordination behaviour has been reported with effects of  $\text{H}_2\text{O}$  and  $\text{H}$  coadsorption for Pt(1 0 0)/CO [39] and Pt(1 1 1)/CO [40]. The formation of CO islands on Pt, induced by water coordination has been reported [41,42]. The same authors reported that a mixed  $\text{H}_2\text{O}/\text{CO}$  surface phase is formed on Rh(1 1 1), owing to hydrophilic coadsorption. The formation of segregated vs. mixed CO/H adlayers on Pt and Rh(1 0 0) and (1 1 0) as a function of electrode history has also been noticed [43].

Lower values of  $A + B_{\text{BE}}$  can thus be explained with a lower adsorption energy. Smaller  $C$  values seem to be due both to a more limited degree of back-donation (through type-i effects) – which is likely to be connected with a less bound configuration – and to the coadsorption with the still weaker bound form, related to the formation of surface ionic couples (through type-ii effects). Even though, on the basis of the arguments given in the above paragraph, it is not possible to assign a single mechanism for the changes in Stark-tuning on the basis of FT-IR measurements alone; nevertheless, this quantity can be regarded as a sensitive probe of the variations of the instantaneous electroactivity of Pt-based electrocatalysts for alcohol oxidation.

Fig. 3(2) shows that the peak area – though positively correlated with anodic polarisation in each of the three series of measurements – exhibits a progressive decrease with electrode aging. Of course, this observation can be related to the decrease of surface concentration of electroactive sites, most probably due to the agglomeration processes pinpointed by SEM (Fig. 1).

As one can notice from Fig. 3(3), at variance with the peak position and intensity, the peak width – essentially due to heterogeneous broadening – does not seem to exhibit a definite trend with electrode aging. This result – in conjunction with the information that we derived from Fig. 3(1) and (2) – points to the fact that, in the case at hand, electrocatalyst degradation is related to changes in CO bonding strength and decrease of active site coverage, rather than to the formation of a multiplicity of adsorption sites.

Eventually, as can be noticed particularly in Fig. 2(B) (corresponding to replicate B that probably exhibits a better signal-to-noise ratio than replicate C where catalyst degradation is more emphasised), a second peak at  $2142 \pm 1 \text{ cm}^{-1}$  (not showing a measurable trend in peak position and width with the applied potential, but exhibiting a positive correlation of the peak area with anodic polarisation) tends to show up with electrode aging. To our knowledge – in the case of CO adsorption – this mode was observed only in a few experiments, carried out in gas phase and tentatively

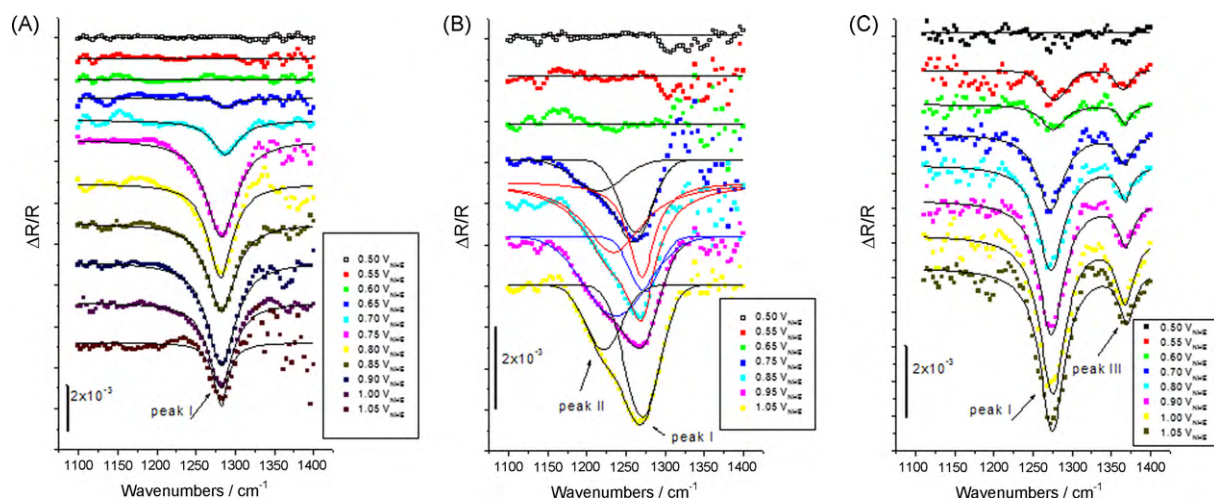


**Fig. 4.** Potential-dependent in situ FT-IR spectra measured at the indicated potentials on a WC/Pt-black electrode in contact with a 0.1 M HClO<sub>4</sub> + 0.1 M CH<sub>3</sub>CH<sub>2</sub>OH solution; reference spectrum measured at 0.05 V<sub>RHE</sub>. Wavenumbers range corresponding to diagnostic modes of ethanol and acetic acid. (A) First sequence, (B) second sequence, and (C) third sequence.

assigned to some “weakly bound” form of CO adsorbed on: oxidised Pt [44] or Pt surface defects [45].

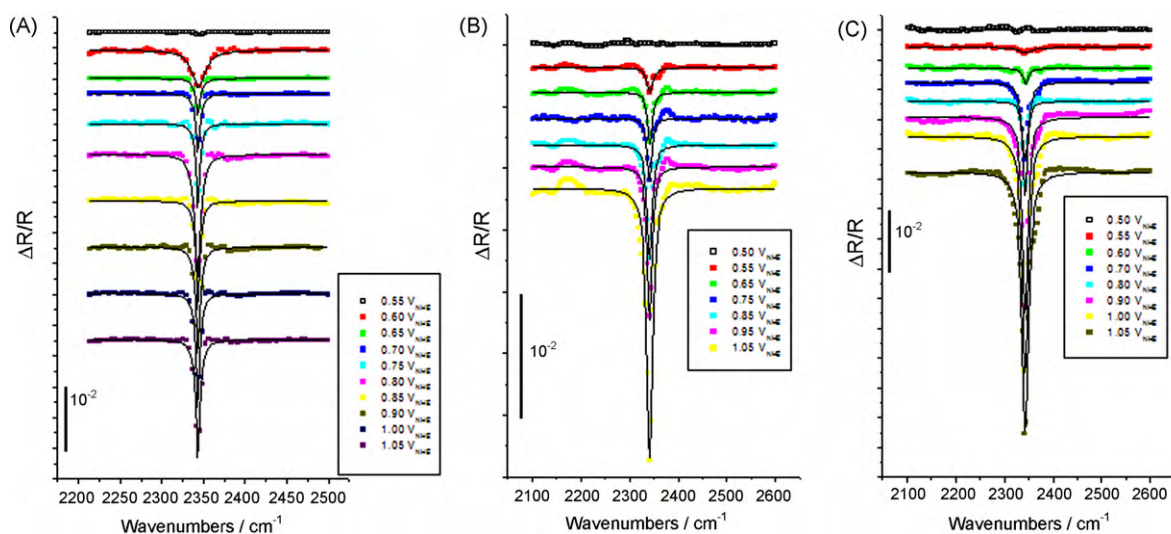
### 3.2. Wavenumber range 1200–1400 cm<sup>-1</sup>

Fig. 4 reports IR spectra in a wavenumber range containing several potentially diagnostic bands corresponding to ethanol and several of its oxidation products. A dominating band centred at ca.  $1270 \pm 80 \text{ cm}^{-1}$  (peak I) – the only actually detectable in series A – is accompanied by a shoulder – corresponding to a band at ca.  $1227 \pm 10 \text{ cm}^{-1}$  (peak II) – in series B and by a second band located at ca.  $1368 \pm 2 \text{ cm}^{-1}$  (peak III) in series C. The band intensities and the slight redshift with anodic potential of the peak at ca.  $1280 \text{ cm}^{-1}$  suggest that these vibrations correspond to adsorbed species. The average position of peak I changes with the replicate potential sequences as follows: A:  $1283 \pm 3 \text{ cm}^{-1}$ , B:  $1270 \pm 5 \text{ cm}^{-1}$ , C:  $1274 \pm 2 \text{ cm}^{-1}$ . The peak widths ( $38.7 \pm 2.4 \text{ cm}^{-1}$ ) and areas ( $-0.17 \pm 0.05$ ) are essentially unaffected by electrode aging. According to the literature, peaks I, II and III can be assigned

as follows: I: C–OH stretching of acetic acid [20]; II: COH–CH<sub>3</sub> combination band that can be assigned to both acetic acid and ethanol [19]; III: coupled C–O stretching and OH deformation of ethanol [19,25]. Notwithstanding the specific differences of surface sensitivity that characterise the two in situ spectroscopies, this scenario is coherent with our SFG results on the same system, showing that electrode aging is correlated with the increase of the relative intensities of ethanol to acetate bands. Coherently with the quantitative outcomes of our analysis of CO adsorption, this result can be explained with a decrease of active site surface concentration upon aging, resulting in the decrease of partial oxidation of ethanol and hence increase of ethanol at the interface.

### 3.3. Aqueous-phase CO<sub>2</sub>

A band at  $2343 \pm 1 \text{ cm}^{-1}$  whose peak position is independent on the electrode aging has been measured (Fig. 5), corresponding to the asymmetric stretching of the O–C–O group of solution-phase CO<sub>2</sub>. Again, coherently with the literature ([19] and references



**Fig. 5.** Potential-dependent in situ FT-IR spectra measured at the indicated potentials on a WC/Pt-black electrode in contact with a 0.1 M HClO<sub>4</sub> + 0.1 M CH<sub>3</sub>CH<sub>2</sub>OH solution; reference spectrum measured at 0.05 V<sub>RHE</sub>. Wavenumbers range typical of CO<sub>2</sub>. (A) First sequence, (B) second sequence, and (C) third sequence.

therein contained). The increasing width (A:  $8.5 \pm 3.9 \text{ cm}^{-1}$ , B:  $12.3 \pm 1.8 \text{ cm}^{-1}$ , C:  $16.1 \pm 7.5 \text{ cm}^{-1}$ ) with electrode aging highlights changes in electroactivity. The trend of peak area with increasing anodic potential within each replicated series is not quantitatively affected by catalyst aging.

#### 4. Conclusions

In this work we have employed in situ FT-IR as a tool for the monitoring of electrocatalyst evolution during prolonged operation: in the present case ethanol oxidation at WC-supported Pt-black. In particular, as a function of anode aging, we monitored the variations of the following bands: (i) stretching of linearly ( $2044\text{--}2063 \text{ cm}^{-1}$ ) and “weakly bonded” ( $2144 \text{ cm}^{-1}$ ) adsorbed CO, (ii) three kinds of bands in the wavenumber range  $1200\text{--}1400 \text{ cm}^{-1}$ , that can be assigned to acetic acid and ethanol and (iii) solution-phase  $\text{CO}_2$  ( $2345 \text{ cm}^{-1}$ ). The chief time-dependent variations in spectral pattern can be briefly described in terms of the following facts: (i) both the peak position and the Stark-tuning of adsorbed CO tend to decrease systematically with electrode aging; the aged electrocatalyst seems to adsorb ethanol preferentially with respect to acetic acid. These results show a progressive decrease of active site surface density and to their deactivation with aging and enable a quantitative assessment of the nature of these degradation processes.

#### References

- [1] B. Bozzini, G.P. De Gaudenzi, B. Busson, Ch. Humbert, C. Six, A. Gayral, A. Tadjeddine, *J. Power Sources* 195 (2010) 4119–4123.
- [2] D.R. McIntyre, G.T. Burstein, A. Vossen, *J. Power Sources* 107 (2002) 67–73.
- [3] G. Lu, J.S. Cooper, P.J. McGinn, *J. Power Sources* 161 (2006) 106–114.
- [4] C.D.A. Brady, E.J. Rees, G.T. Burstein, *J. Power Sources* 179 (2008) 17–26.
- [5] H. Chhina, S. Campbell, O. Kesler, *J. Power Sources* 164 (2007) 431–440.
- [6] F.P. Hu, P.K. Shen, *J. Power Sources* 173 (2007) 877–881.
- [7] C. Bianchini, P.K. Shen, *Chem. Rev.* 109 (2009) 4183–4206.
- [8] H. Meng, P.K. Shen, *Chem. Commun.* (2005) 4408–4410.
- [9] Z. Hu, M. Wu, Z. Wei, Sh. Song, P.K. Shen, *J. Power Sources* 166 (2007) 458–461.
- [10] M. Nie, H. Tang, Z. Wei, S.P. Jiang, P.K. Shen, *Electrochem. Commun.* 9 (2007) 2375–2379.
- [11] F. Hu, G. Cui, Z. Wei, P.K. Shen, *Electrochem. Commun.* 10 (2008) 1303–1306.
- [12] C. Paoletti, A. Cemmi, L. Giorgi, R. Giorgi, L. Pilloni, E. Serra, M. Pasquali, *J. Power Sources* 183 (2008) 84–91.
- [13] H.R. Colón-Mercado, B.N. Popov, *J. Power Sources* 155 (2006) 253–263.
- [14] B. Bozzini, C. Mele, A. Tadjeddine, *J. Cryst. Growth* 271 (2004) 274–286.
- [15] F. Huerta, C. Mele, B. Bozzini, E. Morallón, *J. Electroanal. Chem.* 569 (2004) 53–60.
- [16] B. Bozzini, G. Giovannelli, C. Mele, F. Brunella, S. Goidanich, P. Pedeferrri, *Corros. Sci.* 48 (2006) 193–208.
- [17] S.G. Sen, J. Datta, *J. Electroanal. Chem.* 594 (2006) 65–72.
- [18] S. Park, Y.Y. Tong, A. Wieckowski, M.J. Weaver, *Electrochem. Commun.* 3 (2001) 509–513.
- [19] T. Iwasita, F.C. Nart, in: H. Gerischer, C.W. Tobias (Eds.), *Advances in Electrochemical Science and Engineering*, vol. 4, VCH, Weinheim, 1995, pp. 123–216.
- [20] T. Iwasita, B. Rasch, E. Cattaneo, W. Vielstich, *Electrochim. Acta* 34 (8) (1989) 1073–1079.
- [21] P. Gao, S.C. Chang, Z. Zhou, M. Weaver, *J. Electroanal. Chem.* 272 (1989) 161–178.
- [22] F.H.B. Lima, E.R. Gonzalez, *Electrochim. Acta* 53 (2008) 2963–2971.
- [23] J.F.E. Gootzen, W. Visscher, J.A.R. van Veen, *Langmuir* 12 (1996) 5076–5082.
- [24] E. Antolini, *J. Power Sources* 170 (2007) 1–12.
- [25] T. Iwasita, F.C. Nart, *Prog. Surf. Sci.* 55 (1997) 271–340.
- [26] F. Liu, M. Yan, W. Zhou, Z. Jiang, *Electrochem. Commun.* 5 (2003) 276–282.
- [27] N.M. Markovic, H.A. Gasteiger, P.N. Ross Jr., X. Jiang, I. Villegas, M.J. Weaver, *Electrochim. Acta* 40 (1995) 91–98.
- [28] M.W. Severson, C. Stuhlmann, I. Villegas, M.J. Weaver, *J. Chem. Phys.* 103 (1995) 9832–9843.
- [29] S.-C. Chang, M.J. Weaver, *J. Phys. Chem.* 95 (1991) 5391–5400.
- [30] A.B. Anderson, R. Kötz, E. Yeager, *Chem. Phys. Lett.* 82 (1981) 130–134.
- [31] A.B. Anderson, *J. Electroanal. Chem.* 280 (1990) 37–48.
- [32] M.R. Philpott, P.S. Bagus, C.J. Nelin, H. Seki, *J. Electron Spectrosc. Relat. Phenom.* 45 (1987) 169–175.
- [33] M. Head-Gordon, J.C. Tully, *Chem. Phys.* 175 (1993) 37–51.
- [34] P.S. Bagus, G. Pacchioni, *Surf. Sci.* 236 (1990) 233–240.
- [35] S. Zou, I. Villegas, C. Stuhlmann, M.J. Weaver, *Electrochim. Acta* 43 (1998) 2811–2824.
- [36] P. Hollins, *Surf. Sci. Rep.* 16 (1992) 51–94.
- [37] C.S. Kim, W.J. Tornquist, C. Korzeniewski, *J. Chem. Phys.* 101 (1994) 9113–9121.
- [38] S. Zou, M.J. Weaver, *J. Phys. Chem.* 100 (1996) 4237–4242.
- [39] S.-C. Chang, M.J. Weaver, *J. Phys. Chem.* 94 (1990) 5095–5102.
- [40] S.-C. Chang, M.J. Weaver, *J. Chem. Phys.* 92 (1990) 4582–4594.
- [41] D. Hoge, M. Tüshaus, A.M. Bradshaw, *Surf. Sci.* 207 (1988) L935–L942.
- [42] F.T. Wagner, T.E. Moylan, S.J. Schmieg, *Surf. Sci.* 195 (1988) 403–428.
- [43] L.J. Richter, T.A. Germer, W. Ho, *J. Chem. Phys.* 86 (1987) 477–490.
- [44] A. Holmgren, B. Andersson, D. Duprez, *Appl. Catal. B* 22 (1999) 215–230.
- [45] A. Yee, S.J. Morrison, H. Idriss, *J. Catal.* 191 (2000) 30–45.